Organic Electronics 11 (2010) 969–978

Contents lists available at ScienceDirect

Organic Electronics

journal homepage: www.elsevier.com/locate/orgel

Synthesis and characterization of poly(*N*-alkyloxyarylcarbazolyl-2,7-vinylene) derivatives and their applications in bulk-heterojunction solar cells

Myungkwan Song [a], Jin Su Park [a], Kyung Jin Yoon [a], Chul-Hyun Kim [a], Min Joung Im [a], Jang Soo Kim [a], Yeong-Soon Gal [b], Jae Wook Lee [c,*], Jun Hee Lee [d], Sung-Ho Jin [a,*]

[a] *Department of Chemistry Education, Interdisciplinary Program of Advanced Information and Display Materials, and Center for Plastic Information System, Pusan National University, Busan 609-735, Republic of Korea*
[b] *Polymer Chemistry Lab., Kyungil University, Hayang 712-701, Republic of Korea*
[c] *Department of Chemistry, Dong-A University, Busan 604-714, Republic of Korea*
[d] *Department of Advanced Materials Engineering, Dong-A University, Busan 604-714, Republic of Korea*

ARTICLE INFO

Article history:
Received 10 October 2009
Received in revised form 7 March 2010
Accepted 30 March 2010
Available online 4 April 2010

Keywords:
Poly[*N*-(3,4-bis(decyloxy)phenyl)-carbazolyl-2,7-vinylene]
Bulk-heterojunction solar cell
Gilch polymerization
π-Conjugated polymers

ABSTRACT

The novel π-conjugated polymers, poly(*N*-(3,4-bis(decyloxy)phenyl)carbazolyl-2,7-vinylene) (PCzV) and poly[*N*-(3,4-bis(decyloxy)phenyl)carbazolyl-2,7-vinylene)-*co*-{2-methoxy-5-(2-ethylhexyloxy)-1,4-phenylenevinylene}] (PCzV-*co*-MEH-PPV) were synthesized by using the Gilch polymerization method and their photovoltaic properties were investigated. The newly designed and highly branched polymers, formed from PCzV and PCzV-co-MEH-PPV, are soluble in common organic solvents and easily spin-coated onto indium-tin oxide (ITO) coated glass substrates.

The weight-average molecular weights (M_w) and the polydispersity of the polymers were determined to be in the ranges of 3.86–7.9 × 10^4 and 1.60–2.05, respectively. Bulk-heterojunction solar cells, with ITO/PEDOT:PSS/polymer:$PC_{61}BM/TiO_x$/Al configurations, were fabricated. The solar cell based on PCzV-*co*-MEH-PPV:$PC_{61}BM$ (1:6 wt/wt) displays a higher photovoltaic performance as compared to that produced from PCzV:$PC_{61}BM$ (1:6 wt/wt). The bulk-heterojunction solar cell with PCzV-*co*-MEH-PPV:$PC_{61}BM$ (1:6 wt/wt) has a power conversion efficiency (PCE) of 2.31% (J_{sc} = 6.43 mA/cm^2, V_{oc} = 0.82 V, FF = 44%), measured using an AM 1.5 G solar simulator at 100 mW/cm^2 light illumination.

© 2010 Elsevier B.V. All rights reserved.

1. Introduction

Over the last two decades, new π-conjugated polymers, which have a large number of potential applications in the field of electronic materials, have been developed. π-Conjugated polymers have many advantages over competitive materials that include low cost, easy modification, and solution processability. Various polymers of this type, such as poly(*p*-phenylenes) [1], poly(*p*-phenylenevinylene) (PPV) [2], poly(fluorenes) [3,4], poly(thiophenes) [5,6], and poly(carbazoles) [7,8], have been designed, prepared and investigated. Among these substances, π-conjugated polymers based on poly(carbazoles) have several unique and attractive properties [9,10]. As a result, the hole-transporting [11] and photovoltaic [12,13] properties of poly(carbazoles) have been probed. In these materials, the carbazole nitrogen serves as a site for ready introduction of functionality that can be used to modulate the properties. Moreover, the carbazole starting material is inexpensive and carbazole units can be easily linked to one another through either 2,7- or 3,6-bonds. Since poly(2,7-carbazoles), in contrast to poly(3,6-carbazoles), can have linear structures that possess high degrees of π-conjugation along the backbone,

---

* Corresponding author. Tel.: +82 51 510 2727; fax: +82 51 581 2348.
E-mail addresses: jlee@donga.ac.kr (J.W. Lee), shjin@pusan.ac.kr (S.-H. Jin).

1566-1199/$ - see front matter © 2010 Elsevier B.V. All rights reserved.
doi:10.1016/j.orgel.2010.03.024

they have received particular attention as in the context of bulk-heterojunction solar cells. For example, Morin and co-workers described the synthesis of a variety of new poly(2,7-carbazoles) [14]. In a later effort, the first photovoltaic device derived from poly(*N*-alkyl-2,7-carbazole), which has a power conversion efficiency (PCE) of 0.6%, was described by Müllen and co-workers [15].

In recent years, considerable interest has grown in the area of low-band gap polymers owing to their applications in organic solar cell devices as an active layer for light absorption and charge generation [16–18]. High power conversion efficiencies (PCEs) are key goal for solar applications since these values determine how much electrical energy is produced by absorbed photons. One strategy to improve PCE is to employ well designed and readily synthesized low-band gap polymers, which have improved overlap of the polymer absorption spectrum with the standard solar spectrum under AM 1.5G. One successful approach that has been used to design these polymers takes advantage of vinylene linkages in π-conjugated systems. Based on this design principal, a number of polymers have been prepared which, in comparison to conventional π-conjugated polymers, have low the band gaps in the range of 0.3–0.5 eV [19]. Another advantage arising from the introduction of vinylene units is that it serves as a good method to create planar molecules with extended π-conjugation lengths. This is a consequence of the relatively small dihedral angle that exists between vinylene and aryl groups that leads to an increase in the absorption maxima of the material [20]. Finally, different monomer units can be easily introduced into the polymer in order to fine tune electronic properties.

We have previously described the preparation of novel vinylene based, π-conjugated polymers, including the alkyloxyphenoxy and 1,3,4-oxadiazole-substituted PPVs, poly(9,9-dioctylfluorenyl-2,7-vinylene) (PFV), PFV-*co*-MEH-PPV, highly luminescent poly(*m*-SiPh-PV) derivatives, highly branched poly(PDOT-PV), poly(PDOT-PV-*co*-*m*-SiPh-PV), poly($3OC_1OC_{10}$-PV), and poly($3OC_1O$-C_{10}-PV-*co*-*m*-SiPh-PV) [21–27].

In this effort, repeating vinylene units were introduced between the 2- and 7-positions of the carbazole main chain by using the Gilch polymerization procedure [28]. The substances prepared in this effort include poly(*N*-(3,4-bis(decyloxy)phenyl)carbazolyl-2,7-vinylene) (PCzV) and its copolymer with MEH-PPV segment, poly[*N*-(3,4-bis(decyloxy)phenyl)carbazolyl-2,7-vinylene)-*co*-{2-methoxy-5-(2-ethylhexyloxy)-1,4-phenylenevinylene}] [PCzV-*co*-MEH-PPV]. These polymers possess many attractive properties, such as high molecular weights, low polydispersities and ready purification. To enhance the solubilities and electronic properties of the derived poly(carbazolyl-2,7-vinylene), a meta and para bis-decyloxyphenyl groups were incorporated on the carbazole nitrogen atoms. The addition of vinylene units along the 2,7-carbazole backbone is expected to tune the highest occupied molecular orbital (HOMO) level of π-conjugated polymers as well as improve the electro-optical properties. The preparation of these polymers along with an analysis of their thermal, optical, electrochemical, and photovoltaic properties are described below.

2. Experimental

2.1. General information

^{1}H NMR spectra were recorded on a Varian Mercury Plus 300 MHz spectrometer and the chemical shifts were recorded in ppm units with chloroform as the internal standard. UV–visible and the emission spectra were recorded with a JASCO V-570 and Hitachi F-4500 fluorescence spectrophotometers. Measurements of solid state emissions were carried out by supporting each film on a quartz substrate, which was mounted to receive front-face excitation at an angle of less than 45°. Each polymer film was excited with several portions of the visible light from a xenon lamp. The molecular weight and polydispersity of the polymer were determined by using gel permeation chromatography (GPC) using a PLgel 5 μm MIXED-C column on an Agilent 1100 series liquid chromatography system with THF as an eluent and calibration with polystyrene standards. Thermal analyses were carried out on a Mettler Toledo TGA/SDTA 851, DSC 822 analyzer under N_2 atmosphere at a heating rate of 10 °C/min. Cyclic voltammetry (CV) was carried out in a 0.1 M solution of tetrabutylammonium hexafluorophosphate ($TBAPF_6$) in benzene:acetonitrile (1.5:1 v/v) [29] using a CHI600C voltammetric analyzer at a potential scan rate of 100 mV/s. Each polymer film was applied to a Pt disc electrode (0.2 cm^2) by dipping the electrode into the polymer solution. A platinum wire was used as the counter electrode, and Ag/$AgNO_3$ electrode was used as the reference electrode.

2.2. Materials

Sodium nitrite, copper cyanide, potassium cyanide, catechol, iodine, iodic acid, copper powder, RED-Al, methanesulfonyl chloride, triethylamine, potassium *tert*-butoxide, 4-*tert*-butylbenzyl bromide, tetrahydrofuran (THF), and *N*,*N*-dimethylacetamide were purchased from Aldrich Co. and used without further purification unless otherwise noted. Solvents were dried and purified by fractional distillation over sodium/benzophenone and handled in a moisture-free atmosphere. Column chromatography was performed using silica gel (Merck, 250–430 mesh).

2.3. Synthesis of 2,7-dicyanocarbazole (**4**)

To a solution of 2,7-diaminocarbazole (**3**) (2 g, 10 mmol) and hydrochloric acid (10 mL) in distilled water (100 mL) was added dropwise an aqueous solution of sodium nitrite (1.66 g, 24 mmol). The resulting solution was stirred for 2 h at 0 °C. Aqueous sodium carbonate was added at 0 °C to bring the pH to 7 (solution A). To a solution of copper cyanide (3.63 g, 40.56 mmol) in distilled water was added a solution of potassium cyanide (2.64 g, 40.56 mmol) in distilled water at room temperature (solution B). To this mixture in an ice bath was added solution A at 0 °C. After being stirred overnight at room temperature, the formed precipitate was removed by filtration. The precipitate was washed with distilled water before being repeatedly triturated with acetone. The triturate was concentrated in vacuo to give a solid which was dissolved in ethyl acetate. Filtration followed by concentration of the filtrate gave a crystalline solid which was recrystallized from ethanol to give 0.54 g. Yield: 25%, ^{1}H NMR (acetone-d_6, δ ppm): 11.3 (br, 1H), 8.46–8.43 (d, 2H, aromatic protons), 8.06 (s, 2H, aromatic protons), 7.62–7.59 (d, 2H, aromatic protons). ^{13}C NMR (acetone-d_6, δ ppm): 141.01, 126.10, 123.48, 123.16, 120.16, 116.85, 110.75.

*2.4. Synthesis of 1,2-bis(decyloxy)benzene (**5**)*

To a solution of catechol (15 g, 135 mmol) in 1-bromodecane (83.7 mL, 404.7 mmol) and DMF (150 mL) was added potassium carbonate (74.58 g, 539.6 mmol). The mixture was stirred at 60 °C for 24 h. and concentrated in vacuo to give a residue which was subjected to flash chromatography on silica gel using ethyl acetate:hexane (1:10) as an eluent. This yielded 50.6 g (96%) of **5**. ^{1}H NMR (CDCl$_3$, δ ppm): 6.92 (s, 4H, aromatic protons), 4.05 (t, 4H, α-protons of decyloxy position), 1.93–1.78 (m, 4H, β-protons of decyloxy position), 1.61–1.25 (br, 28H, aliphatic protons), 0.92–0.89 (m, 6H, aliphatic protons). ^{13}C NMR (CDCl$_3$, δ ppm): 149.25, 121.02, 113.97, 69.21, 32.07, 29.68, 29.47, 26.20, 22.84, 14.24.

*2.5. Synthesis of 1,2-bis(decyloxy)-4-iodobenzene (**6**)*

To a solution of 1,2-bis(decyloxy)benzene (**5**) (20 g, 52 mmol) in acetic acid (600 mL) was added water (200 mL) at 40 °C. Sulfuric acid (16 mL) and iodine (6.768 g, 26.67 mmol) were added and the resulting mixture was stirred at 44 °C. Iodic acid (1 g, 5.68 mmol) was added three times during a 40 min period. After cooling, the mixture was extracted with diethyl ether, washed with aqueous sodium carbonate and saturated brine, dried over anhydrous MgSO$_4$ and concentrated in vacuo to give a the crystalline residue which was recrystallized from ethanol to yield 18.65 g (71%) of **6**. ^{1}H NMR (CDCl$_3$, δ ppm): 7.20–7.12 (s, 2H, aromatic protons), 6.64–6.60 (d, 1H, aromatic protons), 3.97–3.88 (t, 4H, α-protons of decyloxy position), 1.83–1.75 (m, 4H, β-protons of decyloxy position), 1.60–1.27 (br, 28H, aliphatic protons), 0.91–0.86 (m, 6H, aliphatic protons). ^{13}C NMR (CDCl$_3$, δ ppm): 149.80, 129.86, 123.68, 122.54, 115.64, 82.63, 69.45, 32.07, 29.52, 29.17, 26.10, 22.86, 14.31.

*2.6. Synthesis of 9-(3,4-bis(decyloxy)phenyl)carbazole-2,7-dicarbonitrile (**7**)*

To a solution of 2,7-dicyanocarbazole (**4**) (1 g, 5 mmol) and 1,2-bis(decyloxy)-4-iodobenzene (**6**) (7.13 g, 13.8 mmol) in *N*,*N*-dimethylacetamide (60 mL) was added copper powder (2 g, 31 mmol) and potassium carbonate (2.1 g, 15 mmol) under a N$_2$ atmosphere. The mixture was stirred at 160 °C for 12 h, diluted with distilled water, and extracted with methylene chloride. The methylene chloride extracts were dried over anhydrous MgSO$_4$ and concentrated in vacuo giving a residue, which was subjected to flash chromatography on silica gel using chloroform as an eluent. This gave 0.56 g (20%) of **7**. ^{1}H NMR (CDCl$_3$, δ ppm): 8.26–8.23 (d, 2H, aromatic protons on carbazole), 7.68 (s, 2H, aromatic protons on carbazole), 7.61–7.58 (d, 2H, aromatic protons on carbazole), 7.13–7.08 (d, 1H, aromatic proton on benzene), 7.02–6.96 (dd, 1H, aromatic proton on benzene), 6.94–6.91(d, 1H, aromatic proton on benzene), 4.16–4.11 (dt, 4H, α-protons of decyloxy position), 1.97–1.80 (m, 4H, β-protons of decyloxy position), 1.57–1.22 (br, 28H, aliphatic protons), 0.92–0.83 (m, 6H, aliphatic protons). ^{13}C NMR (CDCl$_3$, δ ppm): 149.81, 148.05, 141.09, 135.71, 127.53, 122.84, 120.77, 116.91, 116.80, 114.08, 112.82, 105.59, 98.32, 69.48, 32.05, 29.61, 29.30, 26.26, 22.73, 14.30.

*2.7. Synthesis of 9-(3,4-bis(decyloxy)phenyl)carbazole-2,7-dicarboxylic acid (**8**)*

A mixture of 9-(3,4-bis(decyloxy)phenyl)carbazole-2,7-dicarbonitrile (**7**) (2 g, 3 mmol) in ethanol (50 mL) containing sodium hydroxide (30%, 30 mL) was stirred at 110 °C for 24 h. After hydrochloric acid was added to bring the pH below 7, a portion of the water and ethanol were removed by concentration in vacuo. The resulting mixture was stirred at 120 °C for 3 h, cooled and filtered. The precipitate was dried under reduced pressure to yield 1.99 g (94%) of **8**. ^{1}H NMR (DMSO-d_6, δ ppm): 8.43–8.40 (d, 2H, aromatic protons), 7.91–7.87 (d, 4H, aromatic protons), 7.27–7.21 (t, 2H, aromatic protons), 7.16–7.12 (d, 1H, aromatic proton), 4.12–3.96 (dt, 4H, α-protons of decyloxy position), 1.83–1.65 (m, 4H, β-protons of decyloxy position), 1.52–1.09 (br, 28H, aliphatic protons), 0.91–0.0.81 (q, 6H, aliphatic protons). ^{13}C NMR (DMSO-d_6, δ ppm): 177.60, 162.22, 149.53, 147.48, 141.97, 137.67, 130.18, 121.41, 114.56, 109.57, 108.64, 103.25, 96.12, 71.66, 38.16, 28.33, 25.82, 22.58, 18.64, 13.62.

*2.8. Synthesis of (9-(3,4-bis(decyloxy)phenyl)carbazole-2,7-diyl)dimethanol (**9**)*

To a solution of 9-(3,4-bis(decyloxy)phenyl)carbazole-2,7-dicarboxylic acid (**8**) (2 g, 3 mmol) in benzene (90 mL) was added sodium bis(2-methoxyethoxy)aluminum hydride (RED-Al) (18.7 mL, 62.2 mmol). The mixture was stirred at 100 °C for 24 h. Ice-water was added after hydrochloric acid was added to make the solution acidic. Extraction with chloroform gave an extract that was dried over anhydrous MgSO$_4$ and concentrated in vacuo to give a residue which was subjected to flash chromatography on silica gel using chloroform:ethyl acetate (9:1) as an eluent. This gave 1.30 g (68%) of **9**. ^{1}H NMR (CDCl$_3$, δ ppm): 8.11–8.09 (d, 2H, aromatic protons on carbazole), 7.34 (s, 2H, aromatic protons on carbazole), 7.29–7.26 (d, 2H, aromatic protons on carbazole), 7.05–7.04 (m, 2H, aromatic protons on benzene), 6.99–6.98 (d, 1H, aromatic proton on benzene), 4.83–4.81 (d, 4H, –CH$_2$OH), 4.13–3.94 (dt, 4H, α-protons of decyloxy position), 1.94–1.77 (m, 4H, β-protons of decyloxy position), 1.58–1.19 (br, 28H, aliphatic protons), 0.92–0.83 (q, 6H, aliphatic protons). ^{13}C NMR (CDCl$_3$, δ ppm): 167.88, 162.92, 161.15, 142.61, 139.19, 124.08, 122.54, 120.06, 119.12, 112.50, 109.43, 94.32, 66.48, 65.18, 32.10, 29.55, 29.04, 26.15, 22.92, 14.33.

*2.9. Synthesis of 9-(3,4-bis(decyloxy)phenyl)-2,7-bis(chloromethyl)carbazole (**10**)*

To a solution of (9-(3,4-bis(decyloxy)phenyl)carbazole-2,7-diyl)dimethanol (**9**) (1 g, 2 mmol) in methylene chloride (100 mL) was added methanesulfonyl chloride (0.50 mL, 6.48 mmol) and triethylamine (0.90 mL, 6.48 mmol). The resulting mixture was stirred for 48 h at room temperature, diluted with water and extracted with chloroform. The extracts were dried over anhydrous $MgSO_4$ and concentrated in vacuo giving a residue which was subjected to flash chromatography on silica gel using chloroform as an eluent to yield 0.51 g (48%) of **10**. ^1H NMR ($CDCl_3$, δ ppm): 8.12–8.09 (d, 2H, aromatic protons on carbazole), 7.387.26–8.09 (m, 4H, aromatic protons on carbazole), 7.11–7.08 (q, 2H, aromatic protons on benzene), 7.0 (s, 1H, aromatic proton on benzene), 4.80–4.67 (s, 4H, CH_2Cl), 4.14–3.97 (dt, 4H, α-protons of decyloxy position), 1.93–1.82 (m, 4H, β-protons of decyloxy position), 1.57–1.19 (br, 28H, aliphatic protons), 0.99–0.86 (q, 6H, aliphatic protons). ^{13}C NMR ($CDCl_3$, δ ppm): 150.11, 149.02, 142.04, 135.71, 129.66, 122.84, 120.85, 120.77, 119.80, 114.08, 112.82, 110.29, 69.49, 47.33, 32.08, 29.63, 29.31, 26.26, 22.86, 14.31.

*2.10. Synthesis of poly[N-(3,4-bis(decyloxy)phenyl)-carbazolyl-2,7-vinylene)-co-{2-methoxy-5-(2-ethyl-hexyloxy)-1,4-phenylenevinylene}] [PCzV-co-MEH-PPV] (**13**)*

A potassium *tert*-butoxide solution (1.84 mL of a 1.0 M solution in THF) was added dropwise by using a syringe pump over a 15 min period to a 0 °C solution of 9-(3,4-bis(decyloxy)phenyl)-2,7-bis(chloromethyl)carbazole (**10**) (100 mg, 0.15 mmol) and 1,4-bis(chloromethyl)-2-(2-ethylhexyloxy)-5-methoxybenzene (**12**) (51 mg, 0.15 mmol) in freshly distilled THF (12 mL) under N_2 atmosphere. The solution was stirred at 0 °C for 50 min and cooled. End capping was performed by the addition of 3–4 drops of 4-*tert*-butylbenzyl bromide followed by stirring for 15 min at room temperature. The solution was poured into methanol and the precipitate was removed by filtration. After carrying out successive Soxhlet extractions, the polymer was obtained by pouring the solution into methanol. The resulting product 13 (49 mg, 38%) was obtained by drying reduced pressure. ^1H NMR ($CDCl_3$, δ (ppm): 8.19–6.70 (br, 13H, aromatic and vinylic protons), 4.26–3.29 (br, 9H, α-protons of alkoxy position), 2.03–0.86 (br, 53H, aliphatic protons). Anal. Calcd. for PCzV-*co*-MEH-PPV: C, 78.72; H, 9.32; N, 0.21. Found: C, 75.70; H, 9.13; N, 0.17.

The homopolymer, poly(*N*-(3,4-bis(decyloxy)phenyl)-carbazolyl-2,7-vinylene) (PCzV) was synthesized by using a method that is similar to that used to prepare PCzV-*co*-MEH-PPV.

PCzV: 1H NMR ($CDCl_3$, δ ppm): 8.12–7.94 (br, 2H, aromatic protons), 7.57–7.36 (br, 4H, aromatic protons), 7.18–6.79 (br, 5H, aromatic and vinylic protons), 4.23–3.48 (br, 4H, α-protons of decyloxy position), 1.95–0.68 (br, 38H, aliphatic protons). Anal. Calcd. for PCzV: C, 82.85; H, 9.21; N, 2.42. Found: C, 77.96; H, 9.12; N, 2.22.

2.11. Solar cell fabrication and measurements

Bulk-heterojunction solar cells used to measure photovoltaic properties were constructed as follows. Each glass substrate was coated with a transparent ITO electrode (110 nm thick, 10–20 Ω/sq sheet resistance). The ITO-coated glass substrates were ultrasonically cleaned with detergent, deionized water, acetone, and isopropyl alcohol. The layer of 40 nm thick PEDOT:PSS (H.C. Stack, PH500) was spin-coated onto the pre-cleaned and UV-ozone treated ITO substrates. The spin-coated film was baked in air at 150 °C for 30 min. For fabrication of the active layers composed of interconnected networks of electron donor and acceptor, 1,2-dichlorobenzene and chloroform (1:1 wt.%) solutions of the synthesized polymer (10 mg/mL) and $PC_{61}BM$ (15 mg/mL) were shaken at room temperature for 12 h. The polymer and $PC_{61}BM$ blends was then prepared by mixing the two solutions and subsequent shaking for 12 h. Filtration using a 0.45 μm PTFE (hydrophobic) syringe filter gave the polymer blends with a ratio of the electron donor to the $PC_{61}BM$ as an electron acceptor of 1:3, 1:4, 1:5, and 1:6 wt/wt, respectively. The TiO_x precursor solution (1 wt.%) was spin-casted (4000 rpm) onto the active layer with thickness of *ca*. 10 nm and heated at 80 °C for 10 min in air. After being subjected to vacuum (5×10^{-6} Torr), the Al electrodes with thickness around 100 nm were deposited. The top metal electrode area, comprising the active area of the solar cells, was found to be 4 mm^2. Performance of the solar cells were measured using a AM 1.5G solar simulator (Oriel 300 W) at 100 mW/cm^2 light illumination after adjusting the light intensity using Oriel power meter (model No. 70260 which was calibrated using laboratory standards that are traceable to the National Institute of Standards and Technologies, USA). Current density–voltage (*I*–*V*) curves were recorded using a standard source measurement unit (Keithley 236). All fabrication steps and characterization measurements were performed in an ambient environment without a protective atmosphere. Thickness of the thin films was measured using a KLA Tencor Alpha-step IQ surface profilometer with an accuracy of ±1 nm.

3. Results and discussion

3.1. Synthesis and characterization

The synthetic routes used for preparation of the monomer and the polymers are shown in Scheme 1. Syntheses of the poly(carbazolyl-2,7-vinylene) derivatives, although not often straightforward [30], were accomplished starting with 4,4′-dinitro-2-biphenylamine and employing a sequence involving the known intermediates 4,4′-dinitro-2-azidobiphenyl (**1**), 2,7-dinitrocarbazole (**2**), and 2,7-diaminocarbazole (**3**) [31].

In order to introduce chloromethyl units into the 2- and 7-position of carbazole, the dicyano derivative **4** is generated by using a diazotation-cyanide substitution route. To improve the processibility of the poly(carbazolyl-2,7-vinylene) derivatives, the bulky didecyloxyphenyl pendant group is introduced at the nitrogen atom of carbazole

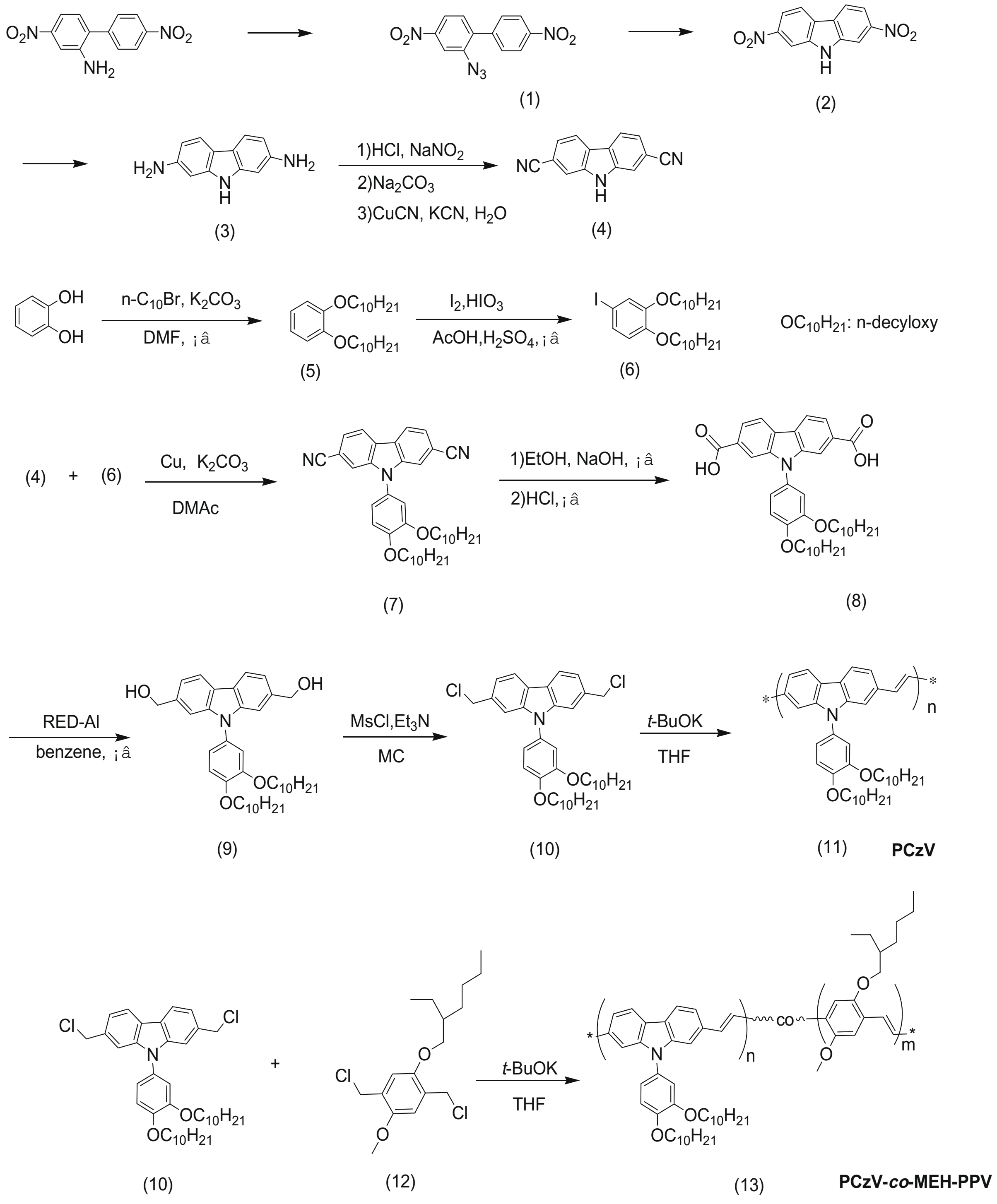

Scheme 1.

backbone. For this purpose, the ortho-hydroquinone derivative **5** is produced by using the Williamson ether synthesis method through reaction of *n*-decyl bromide and catechol. Iodination of **5** yields the iodo-arene **6**, whose coupling reaction with carbazole **4** produces **7**, which contains two decyloxy groups at the *m*- and *p*-positions of the *N*-phenyl position. Hydrolysis of the dicyano compound (**7**) affords the dicarboxylic acid **8**, which undergoes reduction with RED-Al in benzene to yield diol **9**. The corresponding dichloride **10** is then produced from **9** by treatment with methane sulfonyl chloride. PCzV and PCzV-*co*-MEH-PPV are synthesized by using the Gilch polymerization method. Homopolymerization of 9-(3,4-bis(decyloxy)phenyl)-2,7-bis(chloromethyl)carbazole (**10**) and copolymerization with 1,4-bis(chloromethyl)-2-(2-ethylhexyloxy)-5-methoxybenzene (**12**) [32] are carried out with an excess of potassium *tert*-butoxide in dry THF under a N_2 atmosphere. This is followed by the addition of 3–4 drops of 4-*tert*-butylbenzyl bromide in order to end-cap the polymer chain. The polymers, formed in this manner, were found to be completely soluble in organic solvents such as chloroform, 1,2-dichlorobenzene, and THF. The high solubility of these polymers is an important requirement for device fabrication. To improve photovoltaic performance, the resulting polymers were purified by using Soxhlet extraction with different solvents, including methanol, acetone and finally chloroform, in order to remove the unreacted monomers, impurities, and oligomers.

Implementation of this procedure results in the production of highly purified and the narrowly polydispersed polymers. Molecular structures of the monomer and the resulting polymers were characterized by using ^{1}H-, and ^{13}C NMR spectroscopy, and elemental analysis. The chloromethyl protons of monomer **10** at 4.80–4.67 ppm disappear during the polymerization reaction and new vinylic proton resonances appear at 7.18–6.79 ppm together with the carbazole protons in PCzV and PCzV-*co*-MEH-PPV. The composition ratio of PCzV-*co*-MEH-PPV is calculated from the integration ratios of the 8.19–6.70 ppm and 4.26–3.29 ppm peaks in the ^{1}H NMR. ^{1}H NMR peak area calculations show that the actual composition of PCzV-*co*-MEH-PPV is 30:70 wt.%. Table 1 contains a summary of the polymerization results in the form of molecular weight, polydispersity, and thermal characteristics of PCzV and PCzV-*co*-MEH-PPV.

The weight-average molecular weight (M_w) and the polydispersity of the PCzV and PCzV-*co*-MEH-PPV were found to be 38,600, 1.60 and 79,900, 2.05, respectively.

Table 1
Polymerization results, thermal and electro-optical properties of PCzV and PCzV-*co*-MEH-PPV.

		PCzV	PCzV-*co*-MEH-PPV
$M_w \times 10^4$ [a]		3.86	7.99
PDI[a]		1.60	2.05
DSC (T_g)[b]		95	78
TGA[c]		407	377
Abs (nm)	Solution	381,403	489
	Film[d]	386,417	499
PL (nm)	Solution	467,492	556,596
	Film[d]	482,510	585,631
E_g[e] (eV)		2.50	2.07

[a] M_w and PDI of the polymers were determined by GPC using polystyrene standards.

[b] Determined by DSC at a heating rate of 10 °C/min under N_2 atmosphere.

[c] TGA was measured at temperature of 5% weight loss for the polymers.

[d] Measured in the thin film onto the quartz substrate.

[e] Band gap estimated from the onset wavelength of the optical absorption.

3.2. Thermal, optical and electrochemical properties of the polymers

The thermal behaviors of the polymers were investigated by using DSC and TGA thermograms. PCzV and PCzV-*co*-MEH-PPV have glass transition temperatures (T_g) of 95 and 78 °C, respectively, and these polymers have good thermal stabilities with a 5% weight loss temperature at 407 and 377 °C under N_2 atmosphere. PCzV exhibits a higher thermal stability than the PCzV-*co*-MEH-PPV and both polymers have higher thermal stabilities than dialkyloxy-substituted PPVs or poly(9,9-dialkylfluorene)s [33,34]. The high T_g values and thermal stabilities of PCzV and PCzV-*co*-MEH-PPV indicate that these polymers can be used for the fabrication of bulk-heterojunction solar cells without complications associated with deformation or degradation during operation of the solar cells.

Fig. 1 is shown the normalized UV–visible absorption spectra (Fig. 1a) of the PCzV and PCzV-*co*-MEH-PPV in chloroform solutions and in thin films. The absorption spectrum of the PCzV contains two broad peaks at 381 nm and 403 nm in the solution state and at 386 nm and 417 nm in the thin film state. The peaks at *ca.* 400 nm correspond to the carbazole chromophore. The absorption spectrum of the PCzV-*co*-MEH-PPV has a maximum at 489 nm in the solution state and at 499 nm in the thin film state. Both absorption bands in thin film states are slightly red-shifted by *ca.* 10 nm compared to the solution state owing to interactions between the polymer chains. The optical band gaps (E_g), calculated from the onset of the absorption of the PCzV and PCzV-*co*-MEH-PPV, are 2.50 eV and 2.07 eV, respectively. The wavelength of the absorption peaks and the optical band gaps of the PCzV and PCzV-*co*-MEH-PPV are summarized in Table 1. Photoluminescent (PL) spectra of PCzV in chloroform solution and in the thin film state are shown in Fig. 1b. The spectrum of homopolymer PCzV has PL peaks at *ca.* 467 nm and 492 nm in the solution state and at 482 nm and 510 nm in the thin film state. The PL spectrum of the PCzV-*co*-MEH-PPV has maxima at 556 nm and 596 nm in the solution state and at 585 nm and 631 nm in the thin film state. The disappearance of PL emission from PCzV in the PCzV-*co*-MEH-PPV copolymer indicates that efficient energy transfer takes place from the wide band gap PCzV segment to the small band gap MEH-PPV segment. Thus, the transfer of exciton energy from the PCzV segment to the MEH-PPV segment occurs mainly along the polymer chain and intermolecular energy transfer occurs in the PCzV-*co*-MEH-PPV.

To investigate the charge injection and transport properties of PCzV and PCzV-*co*-MEH-PPV and to determine the energies of their highest occupied (HOMO) and lowest unoccupied (LUMO) molecular orbitals, redox measurements were carried using CV. The HOMO energies of PCzV and PCzV-*co*-MEH-PPV for the standard ferrocene/ferrocenium (4.8 eV) are found to be 5.29 eV and 5.34 eV, respectively. The respective LUMO energies, calculated based on the HOMO energies and the band gaps determined by using UV spectroscopic analysis spectra, for PCzV and PCzV-*co*-MEH-PPV are found to be 2.79 eV and 3.27 eV, respectively. The energy band diagrams of PCzV, PCzV-*co*-

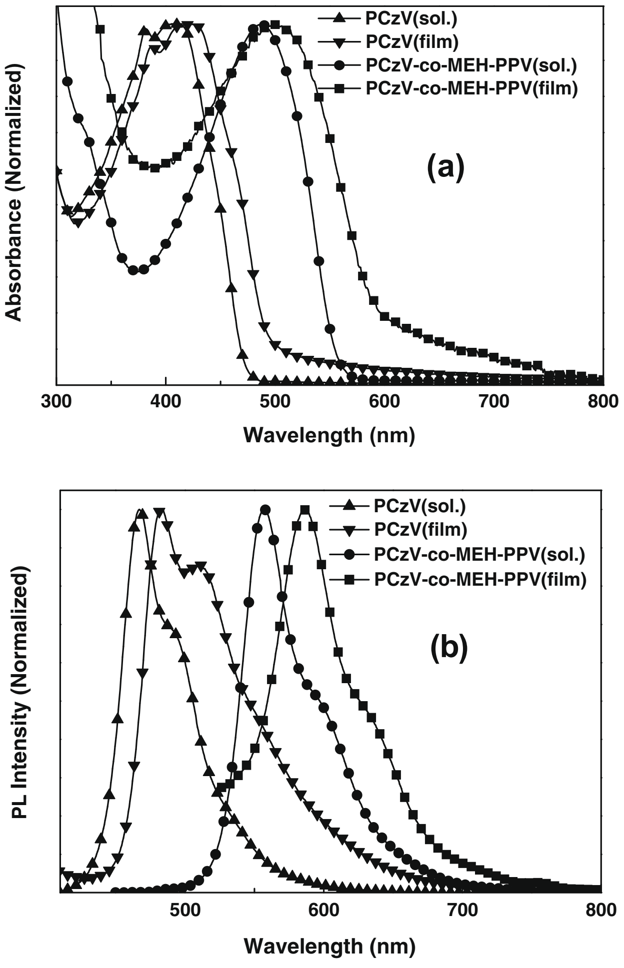

Fig. 1. UV–visible absorption (a) and PL emission (b) spectra of PCzV and PCzV-*co*-MEH-PPV.

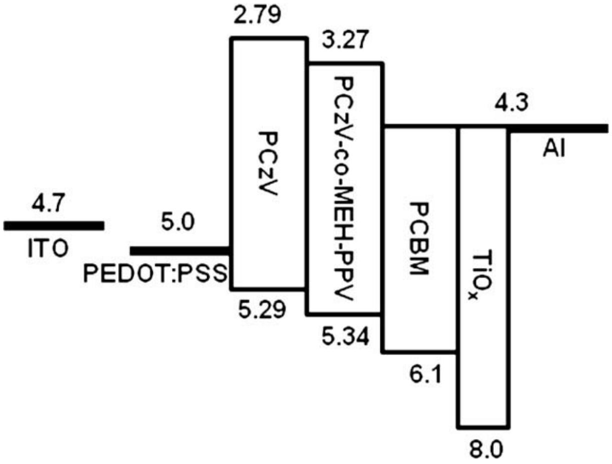

Fig. 2. Energy level diagram of the components of the bulk-heterojunction solar cell.

MEH-PPV and PCBM are shown in Fig. 2. The energies of these electron donors are well-matched to those of $PC_{61}BM$ as an electron acceptor. Photogeneration of charge in most of π-conjugated polymers is not very efficient since there recombination of two charge carriers is always involved. However, a consideration of the high LUMO energies of

PCzV and PCzV-*co*-MEH-PPV and the corresponding low HOMO energy level of $PC_{61}BM$ leads to the prediction that charge transfer will take place at the interface of these materials.

3.3. Solar cell properties of the polymers

Bulk-heterojunction solar cells were fabricated using PCzV and PCzV-*co*-MEH-PPV as electron donors and $PC_{61}BM$ as an electron acceptor. The photovoltaic cell structures are as follow: ITO/PEDOT:PSS/polymer:$PC_{61}BM$/TiO_x (10 nm)/Al (100 nm). We also used solution processable TiO_x [35–37] between the active layer and the metal cathode as a hole blocking and electron transporting layer [38,39]. The energy level of TiO_x matches the work function of Al well. Many research groups have obtained best photovoltaic performances through optimization of the ratios of electron donor polymers to the electron acceptor $PC_{61}BM$ [40,41]. The charge balance generally depends on the thickness of the active layer and the amount of $PC_{61}BM$ in the polymer blended active layer. In this effort, we probed the effect of the ratios of PCzV and $PC_{61}BM$ on photovoltaic performance using a 1,2-dichlorobenzene and chloroform mixed solvent system. The current density–voltage (*J*–*V*) characteristics of solar cells, fabricated with 1:3, 1:4, 1:5 and 1:6 ratios of polymer to $PC_{61}BM$, under AM 1.5G illumination, are shown in Fig. 3 and summarized in Table 2.

Fig. 3a is shown the *J*–*V* characteristics of PCzV with different ratios of $PC_{61}BM$. Open-circuit voltages (V_{oc}) of bulk-heterojunction solar cells are closely related to the energy difference between the HOMO level of the electron donor and the LUMO level of the electron acceptor. The V_{oc} of all solar cells we constructed are almost identical, but higher short-circuit current densities (J_{sc}) and a higher fill factors (FF) are observed with increasing $PC_{61}BM$ content in the blended active layer. The best photovoltaic performance of 0.57% was seen for a solar cell fabricated using a 1:6 ratio of PCzV:$PC_{61}BM$. For reference, the PCE of a cell made using a 1:3 ratio of PCzV:$PC_{61}BM$ (1:3 wt/wt) is 0.26%.

Table 2
Solar cell performance of PCzV and PCzV-*co*-MEH-PPV as electron donor sand $PC_{61}BM$ as the electron acceptor in ITO/PEDOT:PSS/polymer:$PC_{61}BM$/TiO_x/Al devices.

Active layer (polymer:$PC_{61}BM$)	V_{oc} (V) [a]	J_{sc} (mA/cm^2)[b]	FF (%)[c]	PCE (%)[d]
PCzV:$PC_{61}BM$ (1:3 wt/wt)	0.70	1.47	25	0.26
PCzV:$PC_{61}BM$ (1:4 wt/wt)	0.73	1.72	24	0.30
PCzV:$PC_{61}BM$ (1:5 wt/wt)	0.73	2.22	31	0.51
PCzV:$PC_{61}BM$ (1:6 wt/wt)	0.73	2.31	34	0.57
PCzV-*co*-MEH-PPV:$PC_{61}BM$ (1:3 wt/wt)	0.81	5.16	38	1.60
PCzV-*co*-MEH-PPV:$PC_{61}BM$ (1:4 wt/wt)	0.81	5.46	41	1.81
PCzV-*co*-MEH-PPV:$PC_{61}BM$ (1:5 wt/wt)	0.80	6.52	39	2.04
PCzV-*co*-MEH-PPV:$PC_{61}BM$ (1:6 wt/wt)	0.82	6.43	44	2.31

[a] V_{oc}, open-circuit voltage.
[b] J_{sc}, short-circuit current density.
[c] FF, fill factor.
[d] PCE, power conversion efficiency.

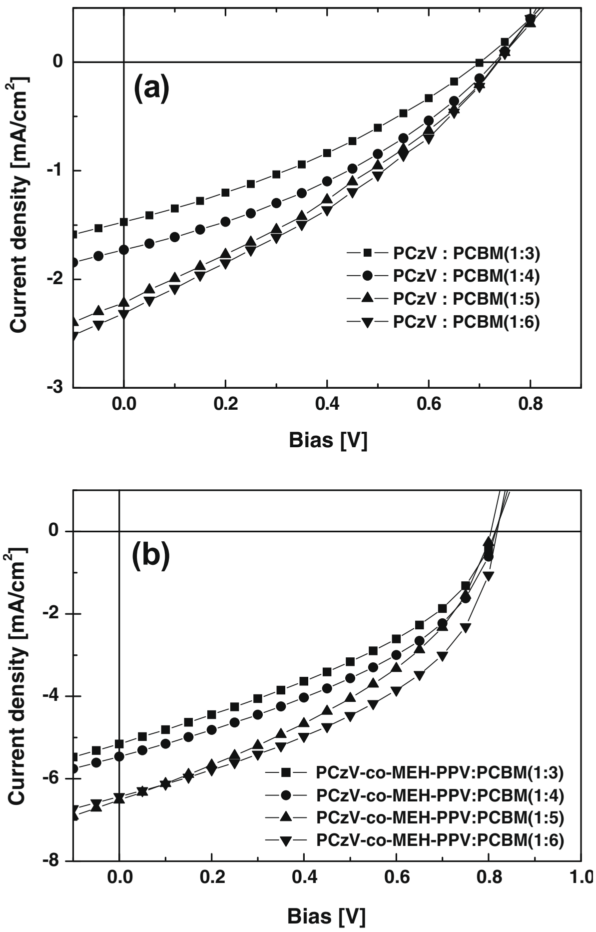

Fig. 3. Current density–voltage characteristic of PCzV (a) and PCzV-*co*-MEH-PPV (b) bulk-heterojunction solar cells containing different ratios of $PC_{61}BM$.

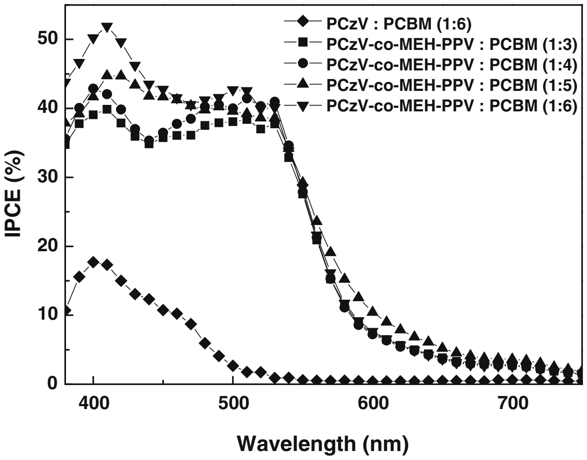

Fig. 4. IPCE spectra of PCzV and PCzV-*co*-MEH-PPV bulk-heterojunction solar cells containing different ratios of $PC_{61}BM$.

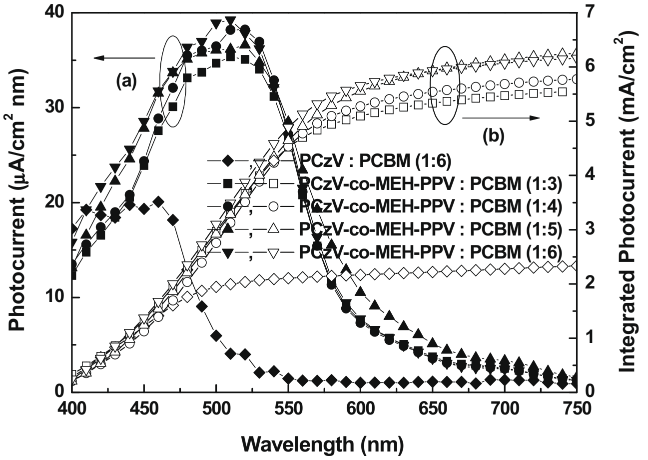

Fig. 5. (a) Photocurrents obtained using data from Fig. 4. (b) The total solar photocurrent obtained by integrating the curves shown in plots a.

Owing to the higher energy difference (1.04 eV) between the HOMO of PCzV-*co*-MEH-PPV and LUMO of $PC_{61}BM$ relative to that of PCzV and $PC_{61}BM$ (0.99 eV), the V_{oc} of PCzV-*co*-MEH-PPV:$PC_{61}BM$ solar cells are higher than those of the PCzV:$PC_{61}BM$ solar cells. The PCzV-*co*-MEH-PPV:$PC_{61}BM$ derived solar cells have similar photovoltaic performances as the PCzV:$PC_{61}BM$ cells (see Fig. 3b). The solar cell fabricated with 1:6 ratio of PCzV-*co*-MEH-PPV and $PC_{61}BM$, with TiO_x with V_{oc} of 0.82 V, J_{sc} of 6.43 mA/cm^2, FF of 44%, and PCE of 2.31%, displays the highest photovoltaic performance when compared with the solar cells arising from PCzV and $PC_{61}BM$.

Incident photon to current conversion efficiency (IPCE) spectra of the bulk-heterojunction solar cells fabricated with PCzV-*co*-MEH-PPV and $PC_{61}BM$ as active layers, recorded in the wavelength region between 380 nm and 750 nm, are shown in Fig. 4. In IPCE spectra of bulk-heterojunction solar cells, the shape of peak around 400 nm was enhanced with increasing amount of the $PC_{61}BM$. In order to easily understand, we measured absorption spectra of the PCzV-*co*-MEH-PPV, $PC_{61}BM$ and PCzV-*co*-MEH-PPV:$PC_{61}BM$ solutions (see Fig. S1). $PC_{61}BM$ showed a strong absorption peak at 340 nm and small peaks located at 400–600 nm. However as increasing the blending ratio of $PC_{61}BM$ content in PCzV-*co*-MEH-PPV and $PC_{61}BM$ solutions, the strong absorption peak of $PC_{61}BM$ showed at 340 nm and the absorption peak of PCzV-*co*-MEH-PPV was gradually reduced. It should be indicated that this makes it possible for the $PC_{61}BM$ molecules to penetrate into the PCzV-*co*-MEH-PPV polymer chains. Thus, the peak in IPCE spectra around 400 nm arises from the absorption of $PC_{61}BM$ and PCzV-*co*-MEH-PPV. As increasing the $PC_{61}BM$ content, more $PC_{61}BM$ molecules are embedded into the PCzV-*co*-MEH-PPV polymer chains, which was in favor of the generation and transport of charge carriers in the $PC_{61}BM$ phase. A maximum IPCE of 17% was observed in the case of the pristine PCzV homopolymer bulk-heterojunction solar cell at a wavelength of 410 nm. As increasing the MEH-PPV content in PCzV-*co*-MEH-PPV copolymers, IPCE also increases considerably and reaches a maximum of 52% at 410 nm and broadened up to 650 nm for a bulk-heterojunction solar cell comprised of a 1:6 ratio (wt/wt) of PCzV-*co*-MEH-PPV:$PC_{61}BM/TiO_x$. This finding may be a result of an increase of the charge-carrier mobility in the active layer and, thus, an increase in light absorption in the solar cell active layer promoted by a high amount of $PC_{61}BM$. This factor also contributes to the increased PCE of PCzV-*co*-MEH-PPV:$PC_{61}BM$ solar cells.

Integrated photocurrent curves were obtained by integrating IPCE spectra in the wavelength region between 400 nm and 750 nm (see Fig. 5). The J_{sc} value, determined from the overlap integral of the IPCE curve and the standard AM 1.5 G solar emission spectrum, is in excellent agreement with the measured photocurrent density. The error of J_{sc} and the integrated photocurrent is 5–7%, which is in the 5–10% range often seen in these values [42]. Therefore, a negligible spectral mismatch exists between the solar simulator used in this study and standard AM 1.5 G sunlight.

4. Conclusions

A new class of high molecular weight poly(*N*-(3,4-bis(decyloxy)phenyl)carbazolyl-2,7-vinylene) (PCzV) and its copolymers with an MEH-PPV have been prepared by using the Gilch polymerization procedure. PCzV and PCzV-*co*-MEH-PPV exhibit high glass transition temperatures and are easily spin casted onto the ITO substrates. Bulk-heterojunction solar cells with ITO/PEDOT:PSS/polymer:$PC_{61}BM/TiO_x$/Al configurations were fabricated with PCzV and PCzV-*co*-MEH-PPV as electron donors and $PC_{61}BM$ as the electron acceptor. The solar cells are comprised of 1:3, 1:4, 1:5 and 1:6 ratios of polymer to $PC_{61}BM$. The PCE values of the solar cells were found to increase with increasing $PC_{61}BM$ content and a maximum PCE of 2.31% (J_{sc} = 6.43 mA/cm^2, V_{oc} = 0.82 V, FF = 44%) is observed for the cell prepared from a 1:6 ratio (wt/wt) of PCzV-*co*-MEH-PPV:$PC_{61}BM$.

Acknowledgements

This work was supported by the Korea Science and Engineering Foundation (KOSEF) Grant funded by the

Korea Government (MEST) (R11-2008-088-01-003-0) and also by the Korea Energy Management Corporation (KEMCO) under the New and Renewable Energy R&D Grant (2008-N-PV08-02).

Appendix A. Supplementary data

Supplementary data associated with this article can be found, in the online version, at doi:10.1016/j.orgel.2010.03.024.

References

[1] S. Qiu, P. Lu, X. Liu, F. Shen, L. Liu, Y. Ma, J. Shen, Macromolecules 36 (2003) 9823.
[2] A.C. Grimsdale, K.L. Chan, R.E. Martin, P.G. Jokisz, A.B. Holmes, Chem. Rev. 109 (2009) 897.
[3] Q. Pei, Y. Yang, J. Am. Chem. Soc. 18 (1996) 7416.
[4] M. Ranger, D. Rondeau, M. Leclerc, Macromolecules 30 (1997) 7686.
[5] K. Faid, R. Cloutier, M. Leclerc, Macromolecules 26 (1993) 2501.
[6] R.D. McCullough, Adv. Mater. 10 (1998) 93.
[7] J.F. Morin, M. Leclerc, Macromolecules 35 (2002) 8413.
[8] H. Yi, A. Iraqi, M. Stevenson, C.J. Elliott, D.G. Lidzey, Macromol. Rapid Commun. 28 (2007) 1155.
[9] G. Zotti, G. Schiavon, S. Zecchin, J.F. Morin, M. Leclerc, Macromolecules 35 (2002) 2122.
[10] J.V. Grazulevicius, P. Strohriegl, J. Pielichowski, K. Pielichowski, Prog. Polym. Sci. 28 (2003) 1297.
[11] S. Wakim, B.R. A, Y. Tao, M. Leclerc, Polym. Rev. 48 (2008) 432.
[12] N. Blouin, A. Michaud, M. Leclerc, Adv. Mater. 19 (2007) 2295.
[13] N. Blouin, M. Leclerc, Account. Chem. Res. 41 (2008) 1110.
[14] N. Leclerc, A. Michaud, K. Sirois, J.F. Morin, M. Leclerc, Adv. Funct. Mater. 16 (2006) 1694.
[15] J. Li, F. Dierschke, J. Wu, A.C. Grimsdale, K. Müllen, J. Mater. Chem. 16 (2006) 96.
[16] M. Svensson, F. Zhang, S.C. Veenstra, W.J.H. Verhees, J.C. Hummelen, J.M. Kroon, O. Inganäs, M.R. Andersson, Adv. Mater. 15 (2003) 988.
[17] M. Catellani, B. Boselli, S. Luzzati, C. Tripodi, Thin Solid Films 403 (2002) 66.
[18] C.J. Tripodi, C. Winder, N.S. Winder, J.C. Winder, A. Winder, P.A. Winder, R.A.J. Winder, Adv. Funct. Mater. 12 (2002) 709.
[19] A. Winder, J. Winder, Chem. Commun. (1998) 2081.
[20] Y. Winder, J. Winder, Y. Winder, J. Phys. Chem. A 109 (2005) 7197.
[21] J.H. Winder, H.S. Winder, W. Winder, Y.S. Gal, J.H. Park, S.H. Jin, J. Polym. Sci. Part A – Polym. Chem. 38 (2000) 4185.
[22] S.H. Jin, S.Y. Kang, I.S. Yeom, J.Y. Kim, S.H. Park, K.H. Lee, Y.S. Gal, H.N. Cho, Chem. Mater. 14 (2002) 5090.
[23] S.H. Jin, H.J. Jin, J.Y. Kim, K. Lee, S.P. Lee, D.K. Moon, H.J. Lee, Y.S. Gal, Macromolecules 35 (2002) 7532.
[24] S.H. Jin, S.Y. Kang, M.Y. Kim, U.C. Yoon, J.Y. Kim, K.H. Lee, Y.S. Gal, Macromolecules 36 (2003) 3841.
[25] S.H. Jin, M.Y. Kim, J.Y. Kim, K. Lee, Y.S. Gal, J. Am. Chem. Soc. 126 (2004) 2474.
[26] H.S. Jeon, S.K. Lee, E.J. Lee, S.M. Park, S.C. Kim, S.H. Jin, Y.S. Gal, J.W. Lee, C. Im, Macromolecules 40 (2007) 4794.
[27] J.S. Park, M. Song, K.J. Yoon, I.A. Shin, M.J. Lee, T.I. Ryu, S.H. Jin, Y.S. Gal, J.W. Lee, Macromolecules 41 (2008) 6696.
[28] H.G. Gilch, L.J. Wheelwright, Polym. Sci. Part A – Polym. Chem. 4 (1966) 1337.
[29] J.M. Hancock, A.P. Gifford, Y. Zhu, Y. Lou, S.A. Jenekh, Chem. Mater. 18 (2006) 4924.
[30] J.F. Morin, M. Leclerc, D. Adès, A. Siove, Macromol. Rapid Commun. 26 (2005) 761.
[31] J.F. Morin, M. Leclerc, Macromolecules 34 (2001) 4680.
[32] P.L. Burn, A. Kraft, R. Baigent, D.D.C. Bradley, A.R. Brown, R.H. Friend, R.W. Gymer, A.B. Holmes, R.W. Jackson, J. Am. Chem. Soc. 115 (1993) 10117.
[33] C. Xia, R.C. Advincula, Macromolecules 34 (2001) 5854.
[34] J.L. Kim, J.K. Kim, H.N. Cho, D.Y. Kim, C.Y. Kim, S.I. Hong, Macromolecules 33 (2000) 5880.
[35] J.Y. Kim, S.H. Kim, H.H. Lee, K.H. Lee, M. Wanli, G. Xiong, A.J. Heeger, Adv. Mater. 18 (2006) 572.
[36] S.H. Park, A. Roy, S. Beaupre, S. Cho, N. Coates, J.S. Moon, D. Moses, M. Leclerc, K. Lee, A.J. Heeger, Nat. Photon. 3 (2009) 297.
[37] K. Lee et al., Adv. Mater. 19 (2007) 2445.
[38] S. Cho et al., Appl. Phys. Lett. 92 (2008) 063505.
[39] A. Hayakawa, O. Yoshikawa, T. Fujieda, K. Uehara, S. Yoshikawa, Appl. Phys. Lett. 90 (2007) 163517.
[40] W. Ma, C. Yang, X. Yang, K. Lee, A.J. Heeger, Adv. Funct. Mater. 15 (2005) 1617.
[41] G. Li, V. Shrotriya, J. Huang, Y. Yao, Y. Yang, Nat. Mater. 4 (2005) 864.
[42] O.K. Varghese, C.A. Grimes, Sol. Energy Mater. Sol. Cells 92 (2008) 374.